Journal of Electron Spectroscopy and Related Phenomena
Elsevier Publishing Company, Amsterdam – Printed in The Netherlands

ELECTRON IMPACT STUDIES OF AUTOIONIZING STATES IN NEON AND HELIUM

J. COMER and F. H. READ
The Physics Department, Schuster Laboratory, Manchester University (England)
(Received 28 February 1972)

ABSTRACT

A study has been made of autoionizing states in neon in the energy region 42–48 eV by low energy electron impact. Observations have been made of structure due to excitation of these states and also their decay by ejection of electrons. New methods of data collection which isolate these two processes are discussed. Studies of autoionizing states in helium in the region 57–65 eV are also presented.

INTRODUCTION

Autoionizing states in atoms have been investigated by several different methods using excitation by photons (e.g. Madden and Codling[1]), ions (Rudd[2]), high energy electrons (Siegbahn et al.[3]), and low energy electrons (Oda et al.[4]). Excitation with photons and high energy electrons both predominantly result in

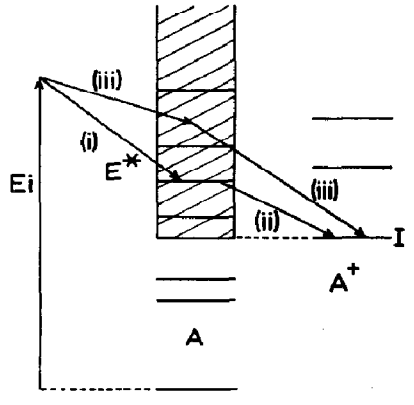

Figure 1. Schematic illustration of three concurrent processes, namely (i) inelastic scattering, (ii) electron ejection and (iii) direct ionization.

optically allowed transitions, whilst excitation with ions and low energy electrons enable the observation of optically forbidden transitions to be made. In the present work we have used electrons having low energies.

In Figure 1 we consider three concurrent processes in the impact of electrons with an atom. These are (i) inelastic scattering leading to bound or autoionizing states, (ii) ejection of electrons from autoionizing states and (iii) direct ionization. When the incident energy is high enough other processes are possible, such as multiple ionizations, or electron ejection from autoionizing states, or multiple electron ejection in Auger processes, etc., but we shall not consider these.

In an experiment in which the spectrum of energies of outgoing electrons is measured, for a constant incident energy E_i, a continuum would be observed due to the direct ionization process and superimposed on this would be two sets of line spectra due to (i) the excitation of autoionizing states giving inelastically scattered electrons of energy $E_i - E^*$ and (ii) their decay giving ejected electrons of energy $E_c = E^* - I$. These two sets of line spectra, which we shall refer to as the "excitation spectrum" and the "ejection spectrum" respectively, may overlap when the incident energy E_i is low. Then one way of distinguishing between them is to make use of the fact that the energies of the inelastically scattered electrons depend on E_i whilst the energies of the ejected electrons do not. It is often essential to do this if one wants to study the electrons ejected from autoionizing states near the threshold of their excitation, and we shall describe convenient experimental methods of completely isolating the spectrum of ejected electrons in such cases.

METHODS OF DATA COLLECTION

We would like to distinguish between four methods of data collection which are illustrated in Figure 2.

(a) This method has previously been used by other workers in this field and in it the incident energy, E_i, is maintained constant and a spectrum is obtained of the yield as a function of energy loss (and therefore of collection energy E_c). A spectrum is taken by changing the collection energy E_c linearly with time and accumulating the yield as a function of time t. That is

$$E_c = E_{c0} + \alpha t$$

where α is a constant such that αt gives the position on the spectrum at t.

Excitation structure is observed at an energy given by

$$E_{c0} + \alpha t = E_i - E^*$$

and emission structure at

$$E_{c0} + \alpha t = E^* - I$$

It is often convenient to employ a spectrum averaging technique in which the collection energy E_c is repeatedly scanned and individual spectra are added together.

(b) This modification of method (a) allows the excitation spectrum to be

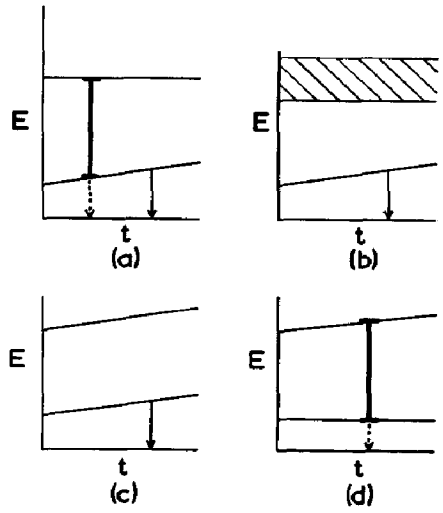

Figure 2. Schematic representation of the four collection schemes. The lower lines represent the variation of collection energy E_c with time t, and the upper lines (or continuous band in the case of scheme (b)) show the variation of the incident energy E_i. The full arrow represents the energy of an ejected electron, and the dashed arrow represents an inelastically scattered electron which has excited the state whose excitation energy is represented by the heavy bar. In scheme (a) both inelastic and ejection structures are seen; in scheme (b) the inelastic lines are present at all times and are therefore averaged out; in scheme (c) the inelastic lines are absent because $E_i - E_c$ does not coincide with an excitation energy; and in scheme (d) the ejection lines are absent because E_c does not coincide with an ejection energy.

effectively removed, leaving only the emission spectrum. Here the yield is measured as a function of collection energy but while the spectrum is accumulating with the spectrum averaging technique the incident energy is changed slowly over a wide range. This means that a particular point on the spectrum is associated with a definite value of ejection energy but with a range of values of energy loss. As a result, although the ejection spectrum is observed as before the excitation spectrum is smeared out. The continuous spectrum due to direct ionization still contributes a smooth background.

(c) The incident energy and collection energy are swept synchronously over the same range.

That is

$$E_i = E_{i0} + \alpha t$$

and

$$E_c = E_{c0} + \alpha t.$$

This maintains the energy loss $(E_i - E_c)$ constant. Ejection structure is again observed at a position on the spectrum given by

$$E_{c0} + \alpha t = E^* - I.$$

A particular feature of this method of data collection is that all the observed lines in the ejection spectrum are excited with the same energy excess $(E_{i0} - E_{c0} - I)$ above their thresholds.

In this method the excitation structure does not appear on the spectrum at all since the fixed energy loss can be chosen to avoid it. If a contribution from excitation structure is still present, however, then any change in the shape of this structure with incident energy will result in a change in the background on the emission spectrum. However this should usually give a relatively smooth variation. Direct ionization processes give a smooth background.

(d) In a similar way to that of case (c) the excitation structure can be observed in isolation from the emission structure by maintaining the observed collection energy constant. The incident energy and energy loss are then varied synchronously to obtain an excitation spectrum. That is

$$E_e = \text{constant}$$

and

$$E_i = E_{i0} + \alpha t.$$

Observed excitation lines are excited at a constant energy, E_e, above their thresholds.

Method (a) can often be used to take either emission or excitation spectra but (b), (c) or (d) should be used to isolate them. Methods (c) and (d) also ensure conveniently that the levels are excited at an energy above threshold which is the same for all lines in a given spectrum. Provided the shapes of the individual lines are not a strong function of incident energy, their shape will be independent of the method used for data collection. However a strong variation in shape with incident energy will result in a modification of the line shape, when methods (b), (c) or (d) are used.

EXPERIMENTAL PROCEDURE

The instrument used for our measurements is of the crossed electron–molecular beam type and many of the experimental techniques and design criteria have been described in a previous paper[5]. Spectra are taken for the target atoms by exciting them with an incident beam of electrons and measuring the yield as a function of the energy of the electrons accepted by the detector. To separate out the ejection electron spectra we have used method (b) since this allows an immediate comparison with the conventional method (a). The collected electron energy is repeatedly scanned and individual spectra are added together, and while the spectrum is accumulating, the incident energy is scanned slowly over a wide range. This results in an ejection spectrum superimposed on a smooth background of the averaged-out excitation spectrum and the direct ionization spectrum.

The resolution with which the excitation of the autoionizing states is observed depends on both the energy spread of the incident beam and the resolution of the energy analyser for the scattered electrons. However the resolution for the ejection structure depends only on that of the analyser, so it is possible to use a much wider spread in the incident beam when only ejection structure is studied.

RESULTS

Experimental results in neon are presented primarily to illustrate the need, discussed in the Introduction, for separating excitation and emission structure. Figure 3 shows spectra obtained in neon. Curves 1 and 2 are energy loss spectra obtained at fixed incident energies of 200 eV and 70 eV (method (a)). They contain energy loss structure due to the excitation of autoionizing states and the energies of these states can be obtained from the excitation energy scale. Curve 3, however, was obtained by method (b), described previously, in which the incident energy was changed in the range 65.0 to 75.0 eV, while the spectrum was accumulating. This shows only emission structure and the energy can be obtained from the emission energy scale.

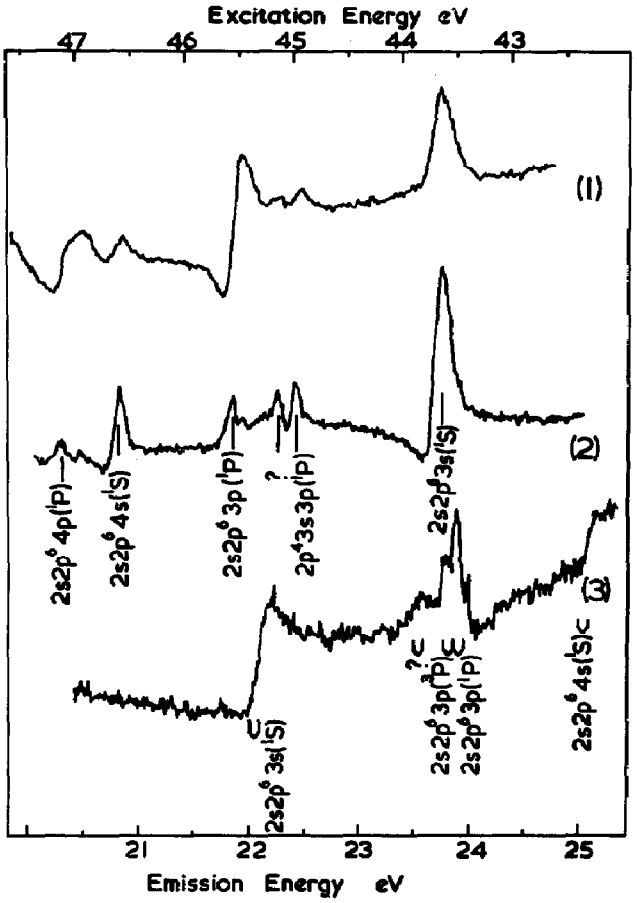

Figure 3. Spectra obtained in neon at a scattering angle of 0° (1) at a fixed incident energy of 200 eV, (2) at a fixed incident energy of 70 eV, and (3) with the incident energy varying in the range 65.0 to 75.0 eV using method (b) (see text). The excitation energy of levels appearing on curves 1 and 2 can be obtained from the upper scale and the ejection energies corresponding to structure in curve 3 can be obtained from the lower scale. The cross-section scale for curve 3 has been multiplied by five with respect to that of curve 2. The structure which appears in curve 3 is actually present in curve 2 but is masked by the larger energy loss structure.

Apart from incident energy, curves 2 and 3 were taken under identical conditions. The structure which appears in curve 3 is actually present in curve 2 but is masked by the larger energy loss structure. Note that the cross-section scale in curve 3 has been expanded by a factor of 5 from that of curve 2.

Figure 4 shows spectra obtained in helium by method (a). At the energies used in this case the observed structure is all due to emission of electrons, and therefore there is no necessity to isolate it in the way that is employed for neon. Figure 5 is an example of a spectrum obtained in helium by method (c) nearer threshold. Here the energy loss was fixed and the incident and emission energy were varied synchronously as described previously. In this case the excitation was carried out 1 eV above the threshold.

In order to calibrate the energy scales a prominent feature was chosen on each spectrum as a reference point. This was then calibrated using energies obtained from photon absorption work. For neon, the calibration was made against the $2s\ 2p^6\ 3p\ (^1P)$ state measured by Codling et al.[6] whilst for helium the $sp\ 22\ (^1P)$ line[1] was used.

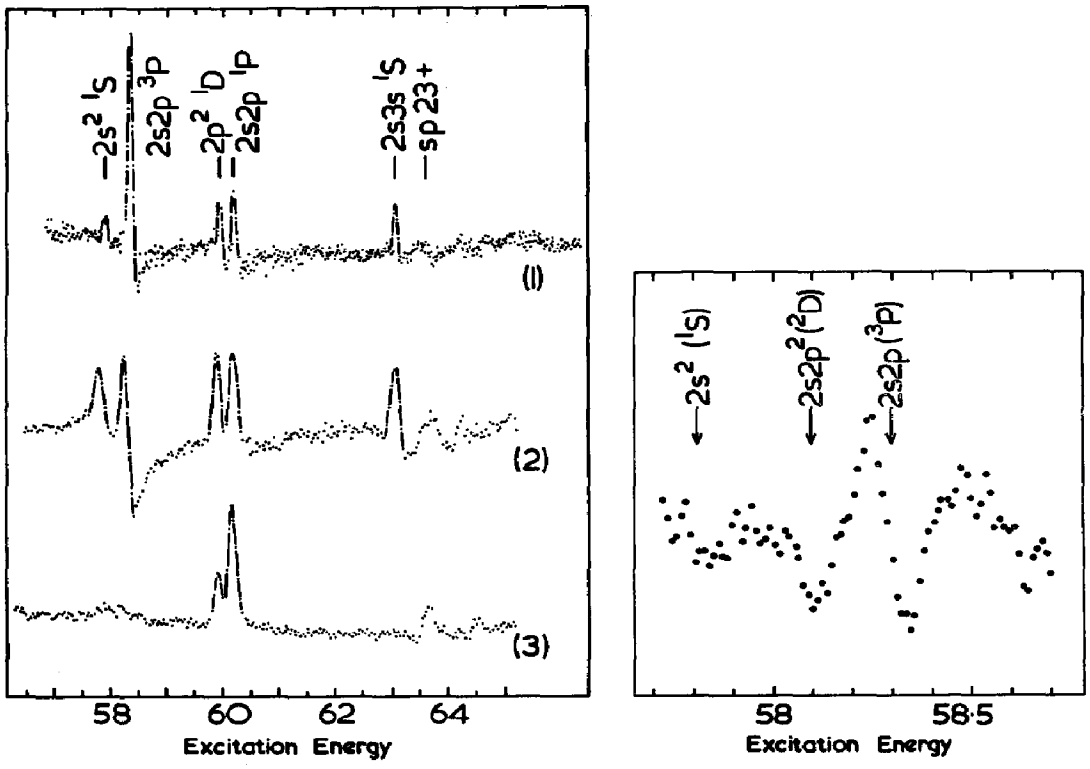

Figure 4 (left). Spectra obtained in helium using method (a) (see text), (1) at an incident energy of 70 eV and a scattering angle of 40°, (2) at an incident energy of 70 eV and a scattering angle of 0°, and (3) at an incident energy of 200 eV and a scattering angle of 0°.

Figure 5 (right). A spectrum obtained in helium using method (c) (see text), showing the yield as a function of incident and collection energy. The energy loss is maintained constant at 25.6 eV.

It was first necessary to assign the calibration points and in each case a sufficient number of previously observed levels were present to make this assignment unambiguously.

DISCUSSION OF RESULTS

Most of the lines observed in the neon spectra in Figure 3 have been assigned to previously observed levels. These have been observed by photon absorption[6], high energy electron impact[3] and by ion impact[7]. The configurations of the autoionizing states responsible are indicated on the diagram. When observed in emission, each level is split into two by decay to the $2s^2\ 2p^5\ (^2P_{\frac{1}{2}})$ and $2s^2\ 2p^5\ (^2P_{\frac{3}{2}})$ final states. If the energy scale of one of the curves 2 and 3 is reversed with respect to the other, a correspondence can be drawn between the excitation of the autoionizing states in curve 2 with their decay in curve 3. If this is done it can be seen that the excitation lines are all prominent in emission with the exception of the $2p^4\ 3s\ 3p\ (^1P)$ which is observed only in excitation. The $2s\ 2p^6\ 3p\ (^3P)$ state appears only in the emission spectrum. This level has previously only been observed by ion impact[7].

In the neon spectra a further level is observed at 45.15 eV which does not appear to have been seen before. We have tentatively assigned this as $2p^4\ (^3P)\ 3s\ (^2P)\ 3p\ (^1S)$ or $2p^4\ (^1D)\ 3s\ (^2D)\ 3s\ (^1D)$ but a definite assignment can only be made when further members of this series are observed. It should be noted that this feature appears in spectra 2 and 3 in the same relative position to the other features. This illustrates an attractive feature of our method. When new autoionizing states are observed in emission, the energy of emission is known but there are often several possibilities for the final state. Therefore it may not be possible to determine the energy of the autoionizing state responsible. Our method, however, leaves no doubt that the final level must be the same as that for the other emission lines, otherwise it would not appear in the same relative position on both spectra, but would be displaced by an energy equal to the difference in the energies of the two final levels.

The ejected electrons are energy analysed with an apparatus function which has a full width at half height of 0.06 eV. With the exception of the $2s\ 2p^6\ 3s\ (^1S)$ level, the widths of all the lines observed in neon appear to be limited by the apparatus function. The $2s\ 2p^6\ 3s\ (^1S)$ line in curve 2, however appears to have a width which is comparable with that of the apparatus function and it is therefore possible to obtain an estimate for this width directly. Provided that this structure represents a single line, its shape should be that of a resonance profile convoluted with the apparatus function which approximates to a Gaussian shape. We have computed this broadened profile using resonance shapes with various parameters and the best fit to the observed profile is obtained when the resonance width is 0.09 ± 0.01 eV.

Our observed energies for the levels in neon and their assignments are shown in Table 1.

In the helium spectra in Figure 4 it is possible to assign all the lines to previous-

TABLE 1

OBSERVED AUTOIONIZATION LINES OF NEON

Errors in final figures in parentheses

State	*Energy (eV)*
$2s\ 2p^6\ 3s\ (^1S)$	43.64 (3)
$2p^4\ 3s\ 3p\ (^1P)$	44.97 (2)
	45.13 (2)
$2s\ 2p^6\ 3p\ (^3P)$	45.45 (3)
$2s\ 2p^6\ 3p\ (^1P)$	45.55
$2s\ 2p^6\ 4s\ (^1S)$	46.60 (2)
$2s\ 2p^6\ 4p\ (^1P)$	47.11 (3)

ly observed autoionizing states of helium and these are indicated on the figure. The ^1P states have been observed in photon absorption[1] and all the singlet states in high energy electron excitation[3]. The $2s\ 2p$ triplet states, however, have only been observed in low energy electron excitation[4, 8]. In the present work the pairs of levels $2s^2\ ^1S$, $2s\ 2p\ ^3P$ and $2p^2\ ^1D$, $2s\ 2p\ ^1D$ are well resolved. It is evident from the curves, that the excitation of triplet states is most prominent at low incident energies. This illustrates the effectiveness of low energy electron impact excitation for investigating these levels.

A comparison of the spectra in Figures 4 and 5 shows how strongly the shape of individual lines can be affected on approaching the threshold of their excitation. The $2s\ 2p\ ^3P$ level at 58.3 eV, which is, predominantly, a peak at 11.7 eV above threshold in Figure 4, becomes asymmetric at 1 eV above threshold in Figure 5.

TABLE 2

OBSERVED AUTOIONIZATION LINES OF HELIUM

Errors in final figures in parentheses

	State	*Energy (eV)*
He	$2s^2\ (^1S)$	57.81 (5)
	$2s\ 2p\ (^3P)$	58.30 (3)
	$2p^2\ (^1D)$	59.87 (3)
	$2s\ 2p\ (^1P)$	60.12
	$2s\ 3s\ (^1S)$	62.98 (3)
	$sp\ 23^+\ (^1P)$	63.56 (7)
He^-	$(2s\ 2p^2)\ ^2D$	58.10 (10)

In the spectrum of Figure 5, further structure appears at 58.10 eV. This does not correspond to any known autoionizing state of He and is probably due to interference between a resonant negative ion state and the continuum. This could be the

$2s\ 2p^2\ ^2D$ state of He^- which has been observed in electron transmission[9] and in the ionization efficiency curve of He (ref. 10).

Our observed energies of the levels in helium, and their assignments, are shown in Table 2.

REFERENCES

1 R. P. Madden and K. Codling, *Astrophys. J.*, 141 (1965) 364.
2 M. E. Rudd, *Phys. Rev. Lett.*, 15 (1965) 580.
3 K. Siegbahn et al., *ESCA Applied to Free Molecules*, North-Holland Publ. Co., Amsterdam, 1969.
4 N. Oda, F. Nishimura and S. Tahira, *Phys. Rev. Lett.*, 24 (1970) 42.
5 J. Comer and F. H. Read, *J. Phys. B*, 4 (1971) 368.
6 K. Codling, R. P. Madden and D. L. Ederer, *Phys. Rev.*, 155 (1967) 26.
7 A. K. Edwards and N. E. Rudd, *Phys. Rev.*, 170 (1968) 140.
8 J. A. Simpson, S. R. Mielczarek and J. Cooper, *J. Opt. Soc. Amer.*, 54 (1964) 269.
9 C. E. Kuyatt, J. A. Simpson and S. R. Mielczarek, *Phys. Rev.*, 138 (1965) 385.
10 J. J. Quéméner, C. Paquet and P. Marmet, *Phys. Rev. A*, 4 (1971) 494.